Supplementary Material

1 MODELLING AND SIMULATION OF BASAL GANGLIA-THALAMO-CORTICAL NEURONS

1.1 Modelling STN-GPe-GPi neurons

The dynamics of each STN-GPe-GPi neuron is modelled by current balance equations for the membrane potential: Terman et al. (2002); Bevan and Wilson (1999); Popovych and Tass (2019):

$$C\frac{dV_i}{dt} = -I_{\text{LEAK}} - I_{\text{K}} - I_{\text{Na}} - I_{\text{Ca}} - I_{\text{T}} - I_{\text{AHP}} - I_{\text{syn}} + I_{\text{DBS}} \tag{S1}$$

$$\frac{dx_i}{dt} = (x_\infty - x_i)/\tau_{x_i} \tag{S2}$$

$$\frac{d[\text{Ca}^{2+}]_i}{dt} = \epsilon_1 \left(-I_{\text{Ca}} - I_{\text{T}} - k_{\text{Ca}}[\text{Ca}^{2+}]_i\right), \tag{S3}$$

where C is the membrane capacity, V_i is the membrane potential of the i-th neuron, x_i denotes the gating variables n, h, r and $[\text{Ca}^{2+}]_i$ is the intracellular concentration of calcium. The exact description of the ionic currents $I_{\text{LEAK}}, I_{\text{K}}, I_{\text{Na}}, I_{\text{Ca}}$ and I_{AHP} is given in table S1. The function x_∞ is given by

$$x_\infty = \frac{1}{1 + e^{-(V_i - \theta_x)/\sigma_x}} \tag{S4}$$

for $x = n, m, h, a, r, s$. In the case of STN neurons, the equilibrium state b_∞ in the T-type current has the following form:

$$b_\infty = \frac{1}{1 + e^{(r_i - \theta_b)/\sigma_b}} - \frac{1}{1 + e^{-\theta_b/\sigma_b}} \tag{S5}$$

The voltage-dependent time scale τ_x has the form

$$\tau_x(V_i) = \tau_{x0} + \frac{\tau_{x_1}}{(1 + e^{-(V_i - \theta_{\tau x})/\sigma_{\tau x}})/A_x} \tag{S6}$$

for the STN neurons and $\tau_x(V_i) = \tau$ for GPe and GPi neurons Terman et al. (2002).

The current I_{DBS} in eq. (S1) models deep brain stimulation. It is applied on STN neurons only and it is described according to the form:

$$I_{\text{DBS}} = A_{\text{DBS}} e^{-\frac{(x-x_0)^2 + (y-y_0)^2 + (z-z_0)^2}{\sigma^2}} H(\sin(2\pi t/T_{\text{DBS}}) \cdot (1 - H(\sin(2\pi(t + \delta_{\text{DBS}})/T_{\text{DBS}})). \tag{S7}$$

while in the absence of DBS treatment is: $I_{\text{DBS}} = 0$. The synaptic currents I_{syn} for STN and GP neurons are given in the section 2. The exact values of the parameters for the STN and GPe-GPi currents are given in table S5.

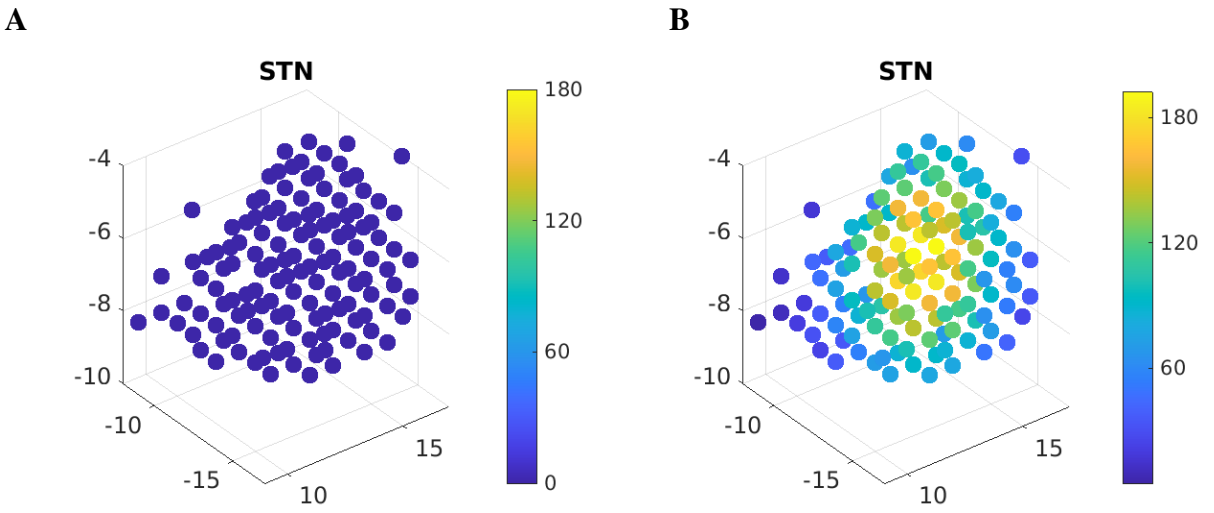

Figure S1. Activation of the STN due to DBS. DBS is modelled by a current which is described in eq. (S7). This type of current is spatially localised at position (x_0, y_0, z_0) and its amplitude decreases exponentially with increasing distance from the source. **A** before excitation i.e. $I_{\text{DBS}} = 0$. **B** During the application of DBS. Here the stimulation centre was set $(x_0, y_0, z_0) = (-13.5, -12, 6.75)$.

Description of current	STN	GPe-GPi
I_{LEAK}	$g_{\text{LEAK}}(V_i - E_{\text{LEAK}})$	$g_{\text{LEAK}}(V_i - E_{\text{LEAK}})$
I_{K}	$g_{\text{K}} n^4 (V_i - E_{\text{K}})$	$g_{\text{K}} n^4 (V_i - E_{\text{K}})$
I_{Ca}	$g_{\text{Ca}} s_\infty^2 (V_i - E_{\text{Ca}})$	$g_{\text{Ca}} s_\infty^2 (V_i - E_{\text{Ca}})$
I_{Na}	$g_{\text{Na}} m_\infty^3 h (V_i - E_{\text{Na}})$	$g_{\text{Na}} m_\infty^3 h (V_i - E_{\text{Na}})$
I_{T}	$g_{\text{T}} a_\infty^3 b_\infty^2 (V_i - E_{\text{K}})$	$g_{\text{T}} a_\infty^3 r (V_i - E_{\text{K}})$
I_{AHP}	$g_{\text{AHP}} \frac{[\text{Ca}^{2+}]}{k_1 + [\text{Ca}^{2+}]} (V_i - E_{\text{K}})$	$g_{\text{AHP}} \frac{[\text{Ca}^{2+}]}{k_1 + [\text{Ca}^{2+}]} (V_i - E_{\text{K}})$

Table S1. The currents for STN-GPe-GPi

Description of current	Tha	MC
I_{LEAK}	$g_{\text{LEAK}}(V_i - E_{\text{LEAK}})$	$g_{\text{LEAK}}(V_i - E_{\text{LEAK}})$
I_{K}	$g_{\text{K}}[(0.75 * (1 - h_i)]^4)(V_i - E_{\text{k}})$	$g_{\text{K}} n^4 (V_i - E_{\text{K}})$
I_{Na}	$g_{\text{Na}} m_\infty^3 h (V_i - E_{\text{Na}})$	$g_{\text{Na}} m^3 h (V_i - E_{\text{Na}})$
I_{T}	$g_{\text{T}} p_\infty^3 (V_i - E_{\text{K}})$	—
I_{M}	—	$g_{\text{M}} p (V_i - E_{\text{K}})$

Table S2. The currents for thalamic and motor cortex neurons.

1.2 Modelling thalamic neurons

The mathematical description of thalamic neurons is given in the following equation:

$$C\frac{dV_i}{dt} = -I_{\text{LEAK}} - I_{\text{K}} - I_{\text{Na}} - I_{\text{T}} - I_{\text{syn}} + I_{\text{SM}} \tag{S8}$$

$$\frac{dx_i}{dt} = (x_\infty - x_i)/\tau_x, \tag{S9}$$

where C is the membrane capacity and V_i is the membrane potential of the i-th neuron, while the eq. (S9) describes the first order kinetics for the gating variables h, r. The forms of the ionic currents I_{LEAK}, I_{K} and I_{Na} and the current I_{T} are given in table S2. The parameter values are listed in table S6. The current I_{SM} represents afferent sensorimotor excitation. For each thalamic neuron, the value I_{SM} is extracted randomly from the interval [0.2, 0.6]. The description of synaptic current I_{syn} in all thalamic neurons is given in section 2.

1.3 Modelling motor cortex neurons

The motor cortex MC neurons are described as one somatic compartment, and follow the equations Pospischil et al. (2008):

$$C\frac{dV_i}{dt} = -I_{\text{LEAK}} - I_{\text{K}} - I_{\text{Na}} - I_{\text{M}} - I_{\text{syn}} + I_{\text{app}} \tag{S10}$$

$$\frac{dx_i}{dt} = a_x(1 - x_i) - b_x x_i \tag{S11}$$

$$\frac{dp_i}{dt} = (p_\infty - p_i)/\tau_p, \tag{S12}$$

where V_i is the membrane potential, and x_i represents the gating variables for potassium and sodium current, of the i-th neuron. The gating variable p_i represents the activation gate of I_{M} current. The form of ionic currents is given in the table S2. For each MC neuron the current I_{app} has different values extracted randomly from the interval [2, 3]. The coefficients a_x, b_x for the gating variable m are described by

$$a_m(V_i) = -0.32\frac{V_i - V_M - 13)}{e^{-(V_i - V_M - 13)/4)} - 1}, \quad b_m(V_i) = 0.28\frac{(V_i - V_M - 40)}{e^{-(V_i - V_M - 40)/5)} - 1} \tag{S13}$$

similar for the gating variable h

$$a_h(V_i) = 0.128e^{-(V_i - V_M - 17)/18}, \quad b_h(V_i) = \frac{4}{1 + e^{-(V_i - V_M - 40)/5}} \tag{S14}$$

and for the gating variable n

$$a_n(V_i) = -0.32\frac{(V_i - V_M - 15)}{e^{-(V_i - V_M - 15)/5)} - 1}, \quad b_n(V_i) = 0.5e^{-(V_i - V_M - 10)/40}. \tag{S15}$$

The equilibrium function p_∞ is given

$$p_\infty(V_i) = \frac{1}{1 + e^{-(V_i + 35)/10}} \tag{S16}$$

with time scale

$$\tau_p(V_i) = \frac{\tau}{3.3e^{(V_i + 35)/20} + e^{-(V_i + 35)/20}} \tag{S17}$$

The motor cortex is modelled as small world network. In this network, 20% of neurons are inhibitory; i.e. they represent interneurons. The cortical neurons show a regular spiking activity Pospischil et al. (2008). The synaptic current description is given in section 2.

2 DESCRIPTION OF THE EXCITATORY AND INHIBITORY SYNAPTIC CONNECTIVITY

Modelling of GPe, GPi, Tha and MC follows a modified small word connectivity. In this modification, each node increases the initial number of connections (or the degree of the node) by $k = 20$ degrees on average. The new contacts lie at a distance less than 5mm (these are the local neighbours); however, the small-world topology Watts and Strogatz (1998) allows remote connections (at a distance greater than 5mm) with a small probability $p = 0.05$. For the STN, the connectivity is described separately in the manuscript. The small-world network is considered in the synaptic currents defined by the activation variable s_i (for the i-th neuron), which are given by Laing and Chow (2002); Ermentrout and Terman (2012); Compte et al. (2000):

$$\frac{ds_i}{dt} = \alpha(1 - s_i)H(V_i - \theta_0) - \beta s_i, \tag{S18}$$

where: $H(V) = \frac{1}{1+e^{-(V-\theta_x)/\sigma_x}}$.

In this paper, we consider excitatory (glutaminergic) and inhibitory (GABA-ergic) synaptic connections. The parameters α, β in eq. (S18) are related to the activation and inactivation time scales, respectively, and have different values for excitatory (glutamatergic) and inhibitory (GABA-ergic) synaptic connections. Specifically, for (glutamatergic) synaptic connections, the values $\alpha = 5, \beta = 1$ are used, and for (GABA-ergic) synaptic connections, the values are $\alpha = 2, \beta = 0.08$.

For each i-th neuron in the network, the synaptic excitation and inhibition, respectively, is described by:

$$I_{i,\text{Glu}} = g_{\text{XY}}(V_i - E_{\text{Glu}}) \sum_j A_{ij} s_j, \tag{S19}$$

with $E_{\text{Glu}} = -10mV$, and

$$I_{i,\text{GABA}} = g_{\text{XY}}(V_i - E_{\text{GABA}}) \sum_j A_{ij} s_j, \tag{S20}$$

with $E_{\text{GABA}} = -70mV$ and the matrix element A_{ij} has the value 1 or 0, depending on whether neurons i and j are connected or not. The summation is taken over all presynaptic neurons. The parameter g_{XY} represents the conductance of the basal ganglia or motor structure X to another basal ganglia or motor structure Y, as listed in tables S5,S3.

In the case of pallido-thalamic connectivity (i.e. from GPi to Tha), our model contains synaptic desensitisation or run-down: GABA-ergic synaptic current changes according to the following function

$$I_{i,\text{GABA}} = g_{\text{XY}}(V_i - E_{\text{GABA}}) \sum_j A_{ij} s_j P_j, \tag{S21}$$

where the factor P_j describes the probability of a neurotransmitter release (in the $\{ij\}$ synapses), and follows the dynamics Benita et al. (2012):

$$\begin{aligned} \frac{dP_j}{dt} &= \frac{P_0 - P_j}{\tau_D} \\ P_j(t_{sp}) &\to P_j(t_{sp}) A_D, \end{aligned} \tag{S22}$$

where t_{sp} corresponds to the last spike-time of the presynaptic neuron, and A_D is the 'depression factor' ($0 < A_D < 1$), in our case, the value $A_D = 0.8$ was used. The value P_0 describes the steady state of P, and in our case was set to 1. To simplify, when a presynaptic neuron fires at time t_{sp} the functionality of the synapse (the release of neurotransmitters) is reduced (suppressed by a factor A_D). In the absence of neural activity the synapse returns to a full release probability, following the time scale $1/\tau$, where $\tau = 400$ ms Benita et al. (2012).

2.1 Modelling the connectivity in the basal ganglia

The coupling between the neurons in the basal ganglia is described by the synaptic current I_{syn}. In the case of STN neurons, the I_{syn} current is given by the summation $I_{\text{syn}} = I_{\text{STST}} + I_{\text{MCST}} + I_{\text{GPST}}$. It indicates the internal excitatory drive between STN neurons, the excitatory drive from MC neurons (via the hyperdirect pathway), and the incoming inhibition from GPe neurons. The excitatory glutaminergic connections within the STN and from MC to STN are expressed by I_{STST} and I_{MCST}, respectively, and follow eq. (S19), while the inhibitory current I_{GPST} is given by eq. (S20) and expresses the inhibition from GPe.

The synaptic current I_{syn} for the GPe region is defined by $I_{\text{syn}} = I_{\text{GPeGPe}} + I_{\text{STGPe}}$, where the first term I_{GPeGPe} expresses the intra-layer inhibitory interaction of GPe neurons (i.e. follows eq. (S20)), while I_{STGPe} describes excitation from STN neurons. For the GPi region the current I_{syn} is given by $I_{\text{syn}} = I_{\text{GPiGPi}} + I_{\text{GPeGPi}} + I_{\text{STGPi}}$, where the first two terms I_{GPiGPi} and I_{GPeGPi} are inhibitory connections, connections from GPi to itself and from GPe to GPi, respectively, while I_{STGPi} describes excitations from STN neurons. The values of the parameters are given in table S5.

2.2 Modelling the connectivity in thalamus and motor cortex

The synaptic current I_{syn} in the thalamus has two components and is given as the summation:

$$I_{\text{syn}} = I_{\text{GPTH}} + I_{\text{THTH}} \tag{S23}$$

where the (GABA-ergic) current I_{GPTH} represents the GABA-ergic inhibition of the GPi area to the thalamus, and for each thalamic neuron has the form of eq. (S21) and eq. (S22). The current I_{THTH} represents the internal excitatory or inhibitory thalamic connections. For each i-th thalamic neuron, the current I_{THTH} has the form:

$$I_{i,\text{THTH}} = g_{\text{THTH1}}(V_i - E_{\text{Glu}}) \sum_j A_{ij} s_j + g_{\text{THTH2}}(V_i - E_{\text{GABA}}) \sum_j A_{ij} s_j \tag{S24}$$

where the element A_{ij} has the value 1 or 0, depending on whether neurons i and j are connected or not. The summations are taken over all presynaptic neurons. In the thalamic area, 20% of the neurons replicate interneurons, i.e., send inhibitory signals (these connections are represented by the second summation of eq. (S24)).

The synaptic current I_{syn} in the motor cortex area has two components and is given as the summation:

$$I_{\text{syn}} = I_{\text{THMC}} + I_{\text{MCMC}} \tag{S25}$$

where the current I_{THMC} represents excitatory connections from the thalamus to the motor cortex area. The current I_{MCMC} represents the internal excitatory or inhibitory motor cortex connections. For each i-th

Description of parameter	Healthy-Normal	Parkinsonian
1. conductance in STN	$g_{\text{STST}} = 0.05$	$g_{\text{STST}} = 1$
2. conductance in GPe	$g_{\text{GPeGPe}} = 0.2$	$g_{\text{GPeGPe}} = 0.07$
3. conductance in GPi	$g_{\text{GPiGPi}} = 0.2$	$g_{\text{GPiGPi}} = 0.07$
4. conductance from STN to GPe	$g_{\text{STGPe}} = 1.96$	$g_{\text{STGPe}} = 3.96$
5. conductance from STN to GPi	$g_{\text{STGPi}} = 5$	$g_{\text{STGPi}} = 8$
6. conductance from GPi to Tha	$g_{\text{GPTha}} = 0.1$	$g_{\text{GPTha}} = .5$
7. current from Striatum to GPi	$I_{\text{app2}} = 0$	$I_{\text{app2}} = 0.1$

Table S3. Differences in the values of the parameters between healthy and Parkinsonian cases.

thalamic neuron, the current I_{MCMC} has two parts in the form:

$$I_{i,\text{MCMC}} = g_{\text{MCMC1}}(V_i - E_{\text{Glu}}) \sum_j A_{ij} s_j + g_{\text{MCMC2}}(V_i - E_{\text{GABA}}) \sum_j A_{ij} s_j \tag{S26}$$

where the element A_{ij} has the value 1 or 0, depending on whether neurons i and j are connected or not. The summations are taken over all presynaptic neurons. In the MC area in our model, 20% of the neurons replicate interneurons, i.e., send inhibitory signals (these connections are represented by the second summation of eq. (S26)).

3 PARAMETER CHANGES BETWEEN HEALTHY AND PARKINSONIAN CONDITIONS

In Parkinson's disease, the degeneration of nigrostriatal dopaminergic neurons leads to a loss of dopamineergic innervation in the striatum. The resulting reduction of D1/D2 receptor-mediated activity affects direct/indirect pathway functionality. In the direct pathway, reduced (D1) receptor activation results in an increase of the GPi neuronal activity as a consequence of disinhibition, which in turn, results in higher levels of inhibitory activity in projections to the thalamus. In the indirect pathway, the reduction of suppressive D2-mediated receptor activation leads to an inhibition of GPe, thus enhancing STN activity. The overactive STN will enhance neuronal activity in the GPi even more - which again leads to even more pronounced thalamic inhibition.

Consistent with this disturbed pathway activation, the model imitates the indirect pathway malfunction by enhancing STN activity and its projection to GPe and GPi. Consequently, in the model we increase the conductance g_{STST}, g_{STGPe}, g_{STGPi} while we decrease the internal GPe and GPi conductance, see table S3. Similar to direct pathway malfunctioning, we assume a decrease in the level of inhibition from striatum to GPi neurons, making GPi neurons overactive. We model this activity by increasing the parameter I_{app2} from 0 to 0.1. Simultaneously, we increase the inhibition from the GPi to the thalamus by increasing the synaptic conductance g_{GPTha}. The above changes are listed collectively in table S3.

Fig. S2 shows the membrane potential changes of one representative neuron from the STN, GPe and GPi, respectively, in all three conditions (i.e. healthy, Parkinsonian and DBS). Fig. S3 depicts one thalamic and one MC neuron from the network, again in healthy, Parkinsonian and DBS conditions.

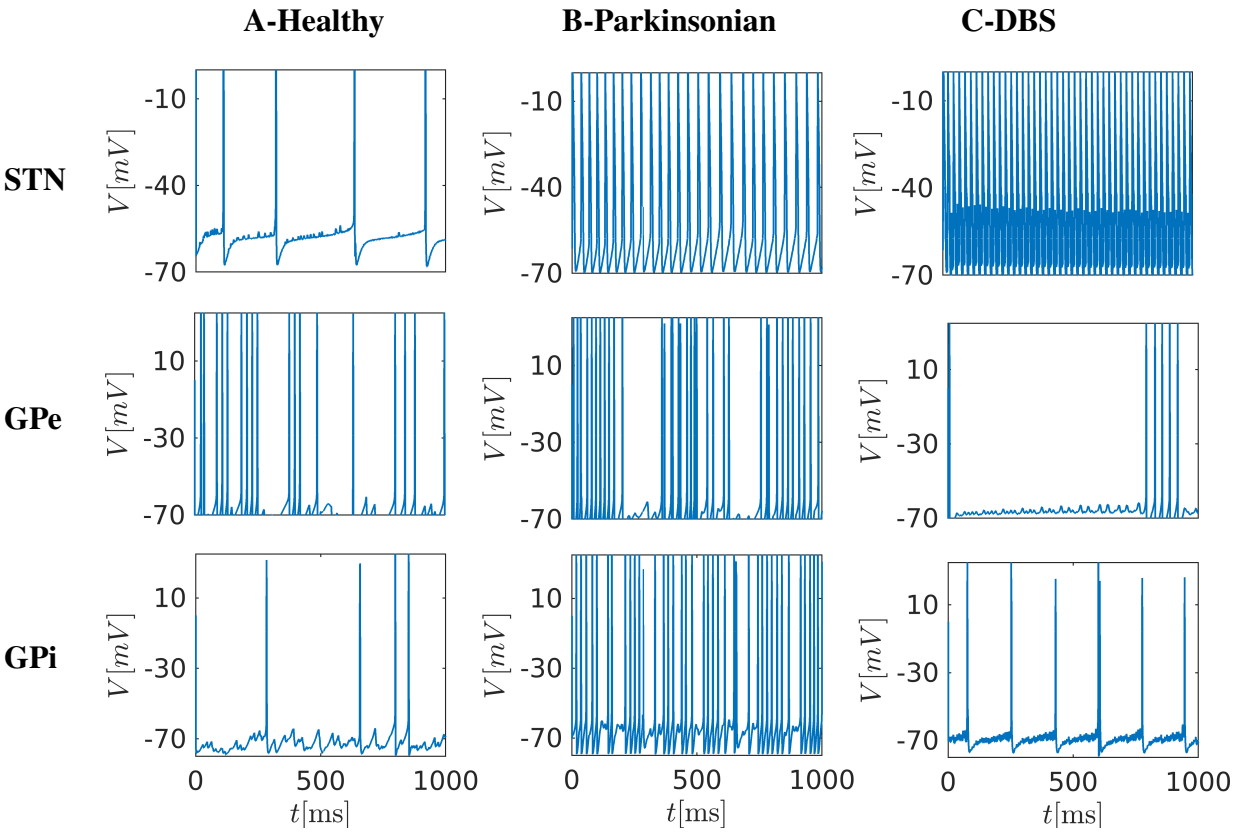

Figure S2. Time series representation of activity of one STN, GPe and GPi neuron each in the network under healthy **(A)**, Parkinsonian **(B)** and **(C)** DBS conditions.

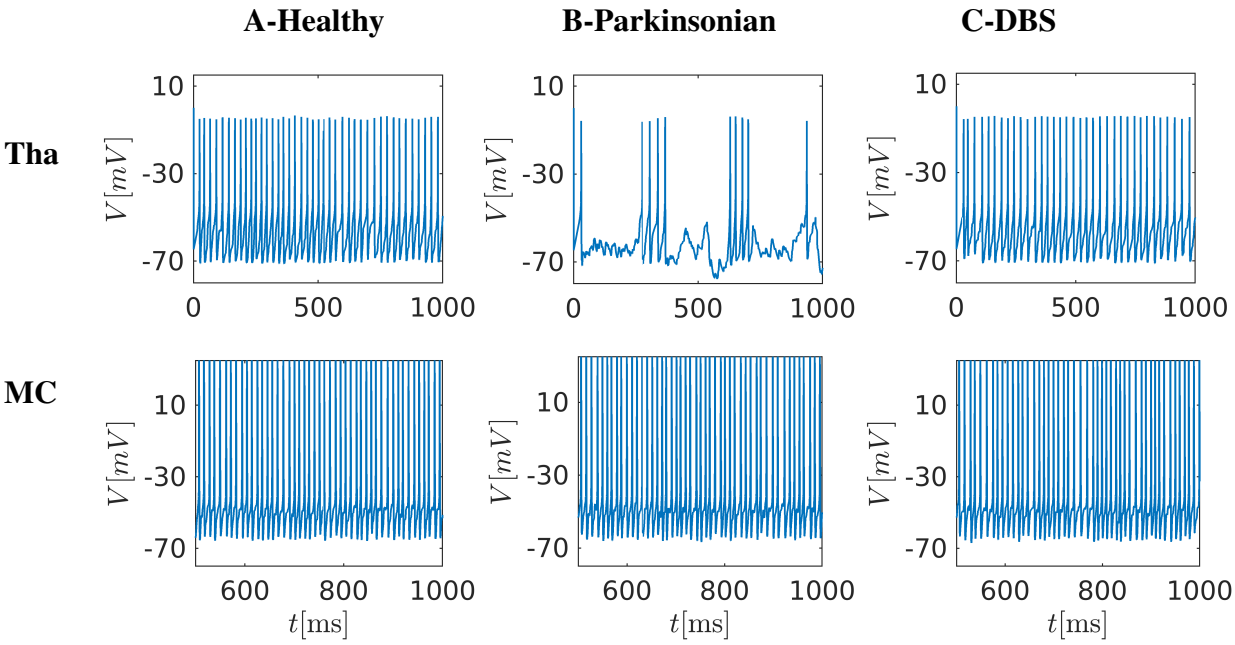

Figure S3. Time series representation of activity of one Tha and one MC neuron in the network under Healthy **(A)**, Parkinsonian **(B)** and **(C)** DBS conditions.

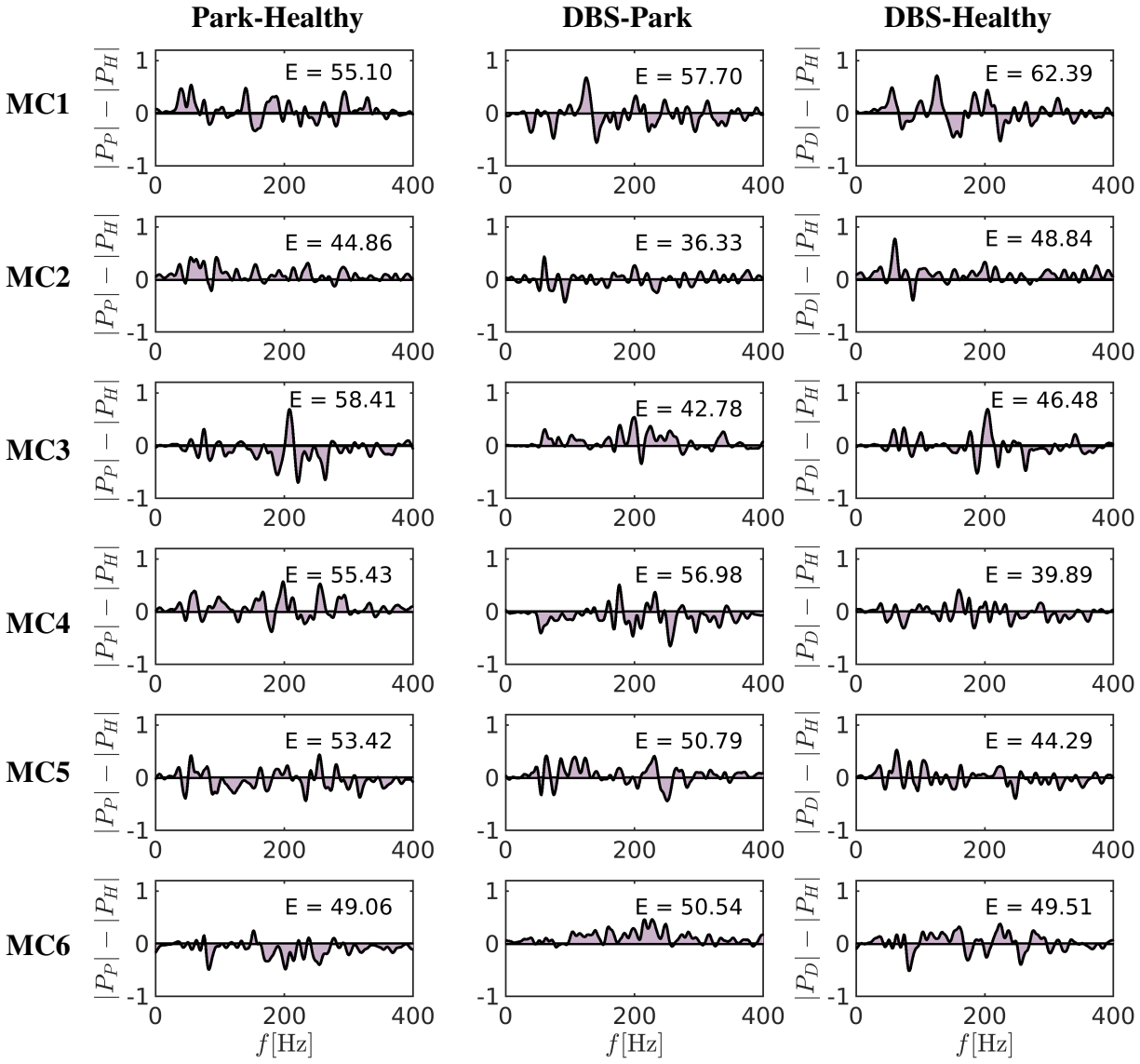

Figure S4. Differences of the spectrum between Park-Healthy and DBS-Healthy (see (S27)). Each row represents one of six cortical sets of nodes as emergent from centrality measure modelling. The columns show the differences of these frequency spectra by subtracting Park vs Healthy, DBSvs Park and DBS vs Healthy. The shaded area under the curve as a measure of frequency spectrum divergence is computed and depicted in columns 1,2 and 3. The MC3, MC4 and MC5 areas in the cases of DBS vs Healthy show a reduction in the computed area compared to Park vs Healthy, indicating that DBS reduces the spectrum difference compared to Parkinsonian condition, although differences to the healthy condition remain.

4 DIFFERENCES IN THE NEURAL ACTIVITY OF MOTOR CORTEX CLUSTERS: PARKINSONIAN-HEALTHY VS DBS-HEALTHY

The network analysis resulted in the identification of six MC high-connectivity areas. In order to estimate the effectiveness of DBS stimulus in these MC areas, we developed the following methodology: We

Motor cortex area	Park-Healthy	DBS-Healthy	Percentage
1. MC1	$E = 55.1$	$E = 62.39$	13.24%
2. MC2	$E = 44.86$	$E = 48.84$	8.9%
3. MC3	$E = 58.41$	$E = 46.84$	-20.4%
4. MC4	$E = 55.43$	$E = 39.89$	-28%
5. MC5	$E = 53.42$	$E = 44.29$	-17%
6. MC6	$E = 49.06$	$E = 49.51$	1%

Table S4. The computed shaded area of Fig. S4 in case of Park vs healthy and DBS vs healthy.

calculated the shaded area which is defined from the quantity $|\,|P_X(f)| - |P_Y(f)|\,|$ and the zero function on the interval [a,b]:

$$E = \int_a^b |\,|P_X(f)| - |P_Y(f)|\,|\,df \tag{S27}$$

where $|P_X|$, $|P_Y|$, are the power spectra of the states X, Y, respectively, and represent: Healthy, Parkinsonian or DBS conditions.

Comparing the difference between Healthy and Parkinsonian conditions (Park-Healthy, see (S27)), one can see that most MC clusters, spectrograms differ by ≈ 55 arbitrary units. Obviously, thus, the effect of Parkinsonian conditions is heterogeneous in the MC network, albeit within moderate boundaries; overall, the difference is in the range of 50 ± 5 (arbitrary units).

Comparing these differences now to differences DBS-Healthy (see (S27)), the relative effect of DBS can be gauged: In two areas, DBS actually induced more differences than the disease condition alone (MC1, MC2, with values of 62.39 and 48.84, compared to 55.1 and 44.86), in three areas, DBS reduces the differences (which might be interpreted as a normalisation of activity), i.e. in MC3, MC4 and MC5 (with values of 46.48, 39.38 and 44.29 compared 58.41, 55.43 and 53.42), and in one area, there is virtually no effect of DBS regarding this measure (MC6, with a value of 49.51, compared to 49.06). Again, this leads to the conclusion that the effect of DBS is heterogeneous regarding cortical activity, with alterations by +18 and +8 $\%$ (positive changes meaning that the frequency spectrogram digresses even more from Healthy conditions under DBS than under Parkinsonian conditions alone) occurring in some regions (MC1, MC2), and -20, -28 and -17 $\%$ in others (MC3, MC4, MC5; negative values indicating that the spectrograms under DBS show less of a difference against Healthy conditions than under Parkinsonian conditions without DBS), and in fact only a minimal change (+0.9 $\%$) in MC6.

Table S5. The following table lists the values of parameters that used for STN and GPe-GPi for mathematical modelling.

STN	value	GPe/GPi	value
g_{LEAK}	2.25 nS/μm^2	g_{LEAK}	0.1 nS/μm^2
g_{K}	45.0 nS/μm^2	g_{K}	30 nS/μm^2
g_{Na}	37.5 nS μm^2	g_{Na}	120 nS/μm^2
g_{T}	0.5 nS/μm^2	g_{T}	0.5 nS/μm^2
g_{Ca}	0.5 nS/μm^2	g_{Ca}	0.15 nS/μm^2
g_{AHP}	9.0 nS/μm^2	g_{AHP}	30.0 nS/μm^2
E_{LEAK}	-60.0 mV	E_{LEAK}	-55.0 mV
E_{K}	-80.0 mV	E_{K}	-80.0 mV
E_{Na}	55.0 mV	E_{Na}	55.0 mV
E_{Ca}	140.0 mV	E_{L}	120.0 mV
τ_{h1}	500.0 ms	τ_{h1}	0.27 ms
τ_{n1}	100.0 ms	τ_{n1}	0.27 ms
τ_{r1}	17.5 ms	τ_{r1}	0.05 ms
τ_{h0}	1.0 ms	τ_{h0}	.05 ms
τ_{n0}	1.0 ms	τ_{n0}	1.0 ms
τ_{r0}	40.0 ms	τ_{r0}	30.0 ms
k_1	15.0	k_1	30.0
k_{Ca}	22.5	k_{Ca}	20
k_2	$3.75 \cdot 10^{-5}$ ms^{-1}	k_2	10^{-4}ms^{-1}
θ_m	-30.0	θ_m	-37
θ_h	-39.0	θ_h	-58
θ_n	-32.0	θ_n	-50
θ_r	-67.0	θ_r	-70
θ_a	-63.0	θ_a	63.0
θ_b	0.4	θ_b	0.4
θ_s	-39.0	θ_s	39.0
$\theta_{\tau h}$	-57.0	$\theta_{\tau h}$	-40.0
$\theta_{\tau n}$	-80.0	$\theta_{\tau n}$	-40.0
$\theta_{\tau r}$	68.0	$\theta_{\tau r}$	-
σ_m	15	σ_m	10
σ_h	-31	σ_h	-12
σ_n	8	σ_n	14
σ_r	-2	σ_r	-2
σ_a	7.8	σ_a	2
σ_b	-0.1	σ_b	-
$\sigma_{\tau h}$	-3	$\sigma_{\tau h}$	-37
$\sigma_{\tau n}$	-26	$\sigma_{\tau n}$	-37
$\sigma_{\tau r}$	-2.2	$\sigma_{\tau r}$	-
A_h	0.75	A_h	0.05
A_n	0.75	A_n	0.05
A_r	0.12	A_r	2
α	5	α	2
β	1	β	0.08
θ_0	-39	θ_0	-57
A_{DBS}	200	-	-
δ_{DBS}	.6 ms	-	-
T_{DBS}	6 ms	-	-

Table S6. The values of parameters that used for Tha and MC are given in the next table.

Tha	value	MC	value
g_{LEAK}	0.05 nS/μm^2	g_{LEAK}	0.1 mS/μcm^2
g_{K}	5 nS/μm^2	g_{K}	5 mS/μcm^2
g_{Na}	3 nS μm^2	g_{Na}	50 mS μcm^2
g_{T}	5 nS/μm^2	g_{M}	0.07 mS/μcm^2
g_{Ca}	0.5 nS/μm^2	g_{Ca}	—
E_{L}	-70.0 mV	E_{L}	-70.0 mV
E_{K}	-90.0 mV	E_{K}	-100.0 mV
E_{Na}	50.0 mV	E_{Na}	50.0 mV
E_{Ca}	140.0 mV	E_{Ca}	—
E_{T}	0 mV	E_{M}	-55 mV
τ_{h1}	500.0 ms	—	—
τ_{n1}	100.0 ms	—	—
τ_{r1}	17.5 ms	—	—
τ_{h0}	1.0 ms	—	—
τ_{r0}	40.0 ms	—	—
k_1	15.0		
θ_h	-41.0		
θ_r	-84.0		
θ_m	-37.0		
θ_p	-60.0		
σ_h	4		
σ_r	4		
σ_m	7		
σ_m	6.2		

REFERENCES

Benita, J. M., Guillamon, A., Deco, G., and Sanchez-Vives, M. (2012). Synaptic depression and slow oscillatory activity in a biophysical network model of the cerebral cortex. *Frontiers in Computational Neuroscience* 6, 64. doi:10.3389/fncom.2012.00064

Bevan, M. and Wilson, C. (1999). Mechanisms underlying spontaneous oscillation and rhythmic firing in rat subthalamic neurons. *Journal of Neuroscience* 19, 7617–7628

Compte, A., Brunel, N., Goldman-Rakic, P., and Wang, X.-J. (2000). Synaptic mechanisms and network dynamics underlying spatial working memory in a cortical network model. *Cerebral Cortex* 10, 910–923

Ermentrout, B. and Terman, D. (2012). *Neural networks as spatio-temporal pattern-forming systems* (New York: Springer)

Laing, C. and Chow, C. (2002). A spiking neuron model for binocular rivalry. *Journal of Computational Neuroscience* 12, 39–53

Popovych, O. and Tass, P. (2019). Adaptive delivery of continuous and delayed feedback deep brain stimulation - a computational study. *Scientific Reports* 9

Pospischil, M., Toledo-Rodriguez, M., Monier, C., Piwkowska, Z., Bal, T., Frégnac, Y., et al. (2008). Minimal hodgkin-huxley type models for different classes of cortical and thalamic neurons. *Biological Cybernetics* 99, 427–441

Terman, D., Rubin, J., Yew, A., and Wilson, C. (2002). Activity patterns in a model for the subthalamopallidal network of the basal ganglia. *Journal of Neuroscience* 22, 2963–2976

Watts, D. and Strogatz, S. (1998). Collective dynamics of 'small-world9 networks. *Nature* 393, 440–442